Some effects of structure on the cure of glycidylether epoxy resins

John M. Barton and David C. L. Greenfield*
Materials & Structures Department, Defence Research Agency, Farnborough, Hampshire GU14 6TD, UK

and K. A. Hodd
Department of Materials Technology, Brunel University, Uxbridge, Middlesex, UK
(Received 6 March 1991; accepted 26 March 1991)

Three glycidylether epoxy resins with functionalities of 2, 3 and 4 were purified and extensively characterized. The cure of the resins with diaminodiphenylsulphone, both alone and as blends, was studied using rheometry and differential scanning calorimetry. The effect of resin functionality on the rate of cure was greater than would be expected from simple concentration effects. The kinetics were best described by an autocatalytic model over approximately the first 40% of reaction. Thereafter an *n*th order expression gave a better fit to the data. The modulus crossover point, $t_{G'=G''}$, was found to be a reproducible indication of gelation, and the fractional conversions at this point, obtained by combining d.s.c. and rheology data, were compared to the values predicted by gelation theory. A model was used to predict the viscosity of samples during cure as an aid to processing.

(Keywords: epoxy; resin; cure; kinetics; viscometry; d.s.c.)

INTRODUCTION

The range of potential applications for epoxy resins is rapidly expanding. They are particularly important as matrix resins for advanced aerospace composites which are being used increasingly in primary aircraft structures. Consequently there is a need both for new resins to supplement those already in commercial use, and for a deeper understanding of the curing process and structure–property relationships of cured resins in order to control the curing effectively and to optimize the properties of the finished product.

Most research programmes to date have concentrated on glycidylamine type epoxy resins, especially tetraglycidyldiaminodiphenylmethane (TGDDM). The only glycidylether resin to be extensively studied is bisphenol-A-diglycidylether (BADGE), shown in *Figure 1a*; indeed one collaborative programme on this resin involved work in four countries[1].

More recently there has been some work on the triglycidylether of tris-(hydroxyphenyl)methane, *Figure 1b*. The studies have mainly involved the monitoring of cure and glass transition temperature (T_g) using torsional braid analysis (t.b.a.)[2,3], water absorption studies, rubber toughening[4,5] and the physical properties of castings[6]. Very little differential scanning calorimetry (d.s.c.) work has been done on this resin[7,8]. There have been no reported studies on a pure, tetrafunctional, glycidylether epoxy resin.

The work described here was part of a larger study of the curing characteristics and structure–property relationships of glycidylether epoxy resins[9]. The objective of this part of the project was to study the cure of glycidylether epoxy resins using complementary calorimetric and rheological methods, with particular emphasis on the effect of resin functionality, and to attempt to predict the cure behaviour as an aid to processing.

EXPERIMENTAL

Materials

The epoxy resins used in this research were: Epon 825 (Shell chemicals); XD7342.02L (Dow Chemical Co.); Epon 1153/114 (Shell Chemicals). The hardener used throughout was 4,4′-diaminodiphenylsulphone (DDS), supplied by Ciba-Geigy Plastics as Hardener HT 976.

The structures of the epoxy resins are shown in *Figure 1*. All were extensively characterized using a range of analytical techniques. The tetrafunctional material shown in *Figure 1c* was obtained in a pure form (94–97% by h.p.l.c.) from crude Epon 1153/114 using preparative scale liquid chromatography. This work is described in detail elsewhere[9].

Curing studies

Sample preparation. Two series of reacting systems were prepared; blending the difunctional Epon 825 (825), with either the trifunctional XD 7342.02L (XD), or the tetrafunctional resin isolated from crude Epon 1153/114 (TF). Their compositions are shown in *Table 1*. Each formulation was mixed with a stoichiometric amount of DDS in an oil bath maintained at 130°C for the minimum time necessary to complete dissolution. After mixing, the samples were stored in sealed bags, in a jar containing silica gel, in a freezer compartment until required for use.

*To whom correspondence should be addressed

0032-3861/92/061177-10

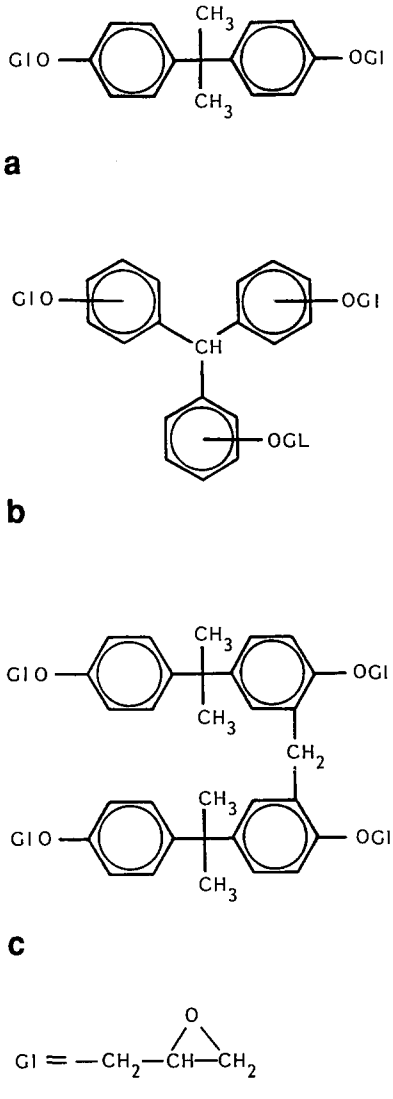

Figure 1 Structures of epoxy resins: (a) Epon 825; (b) XD 7342.02L; (c) Epon 1153/114

Table 1 Composition of resin mixtures

Composition	Mole % 825	Mole % XD	Mole % TF	Average resin functionality
825	100	0	0	2.00
XD25	75	25	0	2.25
XD50	50	50	0	2.50
XD75	25	75	0	2.75
XD100	0	100	0	3.00
TF25	75	0	25	2.50
TF50	50	0	50	3.00
TF75	25	0	75	3.50
TF100	0	0	100	4.00

Rheological measurements. All rheological experiments were carried out using a Rheometrics dynamic spectrometer RDS 7700 fitted with a TC 2000 transducer. Disposable parallel plates with a diameter of 25 mm were used throughout. Preliminary frequency and strain sweeps were carried out to determine optimum experimental conditions.

Isothermal curing experiments were performed on all of the resin formulations using a frequency of 10 rad s^{-1} and a maximum strain of 10%. The environmental chamber of the instrument was pre-heated to 70°C. After equilibrium had been reached the plates were brought together and the gap zero set. The sample was then introduced and the chamber heated rapidly to the preset isothermal cure temperature. It was found that this method was more controlled and reproducible than preheating the whole system to the required cure temperature, and minimized any temperature overshoot. As the cure proceeded, the strain was automatically adjusted to maintain the torque response within the range of the transducer. The viscoelastic properties of the sample during cure, including dynamic viscosity, η^*, shear storage modulus, G', shear loss modulus, G'' and tan delta were monitored.

Other experiments carried out were time sweeps at 10 rad s^{-1} and 10% strain to determine the viscosity of uncured systems, and dynamic curing experiments in which samples of some compositions were heated from 70°C to 150°C at 2°C min^{-1} and then held isothermally.

Differential scanning calorimetry. Calorimetric curing experiments were carried out using a heat flux type DuPont 9900/910 d.s.c. and a Perkin Elmer DSC 7, which operates on the power compensation principle. Both instruments were purged with a continuous flow of nitrogen gas and were calibrated using indium metal supplied by the National Physical Laboratory, Teddington. Temperature scanning experiments were done on the DuPont d.s.c. at a heating rate of 10°C min^{-1} while isothermal runs were carried out using the DSC 7 at temperatures between 145°C and 250°C.

Heat flow, temperature and time were monitored throughout the experiments. After each isothermal run the sample was heated to 260°C for 5 min to complete the reaction and the run was repeated to provide a baseline for reference. The data were then converted into ASCII files and transferred via an RS 232 interface to a Hewlett-Packard HP 86 computer where they were analysed using software developed in-house[10].

RESULTS AND DISCUSSION

Chemorheology

In the initial stages of cure the dynamic viscosity was below the instrument's limit of sensitivity but as the resin cured the log(viscosity) increased linearly with time. At the onset of gelation there was an increase in the gradient and a second linear portion was seen. The shear loss modulus, G'', followed a similarly shaped path. Around the onset of gelation the shear storage modulus, G', increased rapidly and eventually rose above the loss modulus. Tung and Dynes[11] proposed that the point at which the storage and loss modulus curves crossed, i.e. when tan delta = 1, could be taken as an indication of gelation since it represented the point at which the system changed from a viscous liquid to an elastic solid. They reported that gel times measured by this method corresponded closely with those obtained using the standard ASTM test method[12], when a frequency of 10 rad s^{-1} and a low strain were used. Winter[13] has since shown that this is only true for stoichiometric systems at temperatures well above their T_gs, as in the current work.

Each mixture was tested at several different temperatures. In every case an increase in the temperature produced an increase in the rate of reaction as represented

Table 2 Gel times (min) from $t_{G'=G''}$

Composition	825a	XD 25	XD 50	XD 75	XD 100	825b	TF 25	TF 50	TF 75	TF 100
Average resin functionality	2.00	2.25	2.50	2.75	3.00	2.00	2.50	3.00	3.50	4.00
Cure temperature (°C)										
146	105	73	61	51	46	98	74	65	56	55
155	73	50	41	34	33	67	49	44	39	40
165	48	35	29	24	22	46	34	31	28	28
175	35	25	21	–	–	32	24	22	20	20
E (kJ mol^{-1})	59.9	57.0	60.2	57.4	54.7	57.8	59.2	57.2	57.9	58.2

by the gradient of the log(viscosity) curve and a reduction in overall reaction time. At every temperature studied an increasing rate of reaction was seen with increasing resin functionality within each series of blends. Gel times for all blends, determined by the modulus crossover point, $t_{G'=G''}$, are given in *Table 2*. For every mixture, increasing the curing temperature produced a reduction in the gel time. At each temperature, increasing the resin functionality initially produced a very large drop in gel time but each successive increase in functionality led to a smaller decrease in gel time until hardly any difference was discernible between XD 75 and XD 100, or between TF 75 and TF 100. The trifunctional XD 7342.02L and its blends consistently displayed shorter gel times than the tetrafunctional TF and its blends.

Arrhenius plots of $\ln(t_{G'=G''})$ *versus* $1000/T(\mathrm{K})$ are shown in *Figure 2*. Excellent linearity was observed for all formulations confirming that the modulus crossover represented a point of constant fractional conversion. The slope of the plots was $-E/R$ and the activation energies for gelation obtained are given in *Table 2*. In spite of the wide range of reactivities shown by the resin mixtures very little difference was apparent in the activation energies; all falling in the range from 55 to 60 kJ mol^{-1} indicating that the variation in gel time with temperature was independent of the composition of the material under investigation. The high degree of linearity would allow predictions to be made of gel times for cure temperatures outside of the range studied.

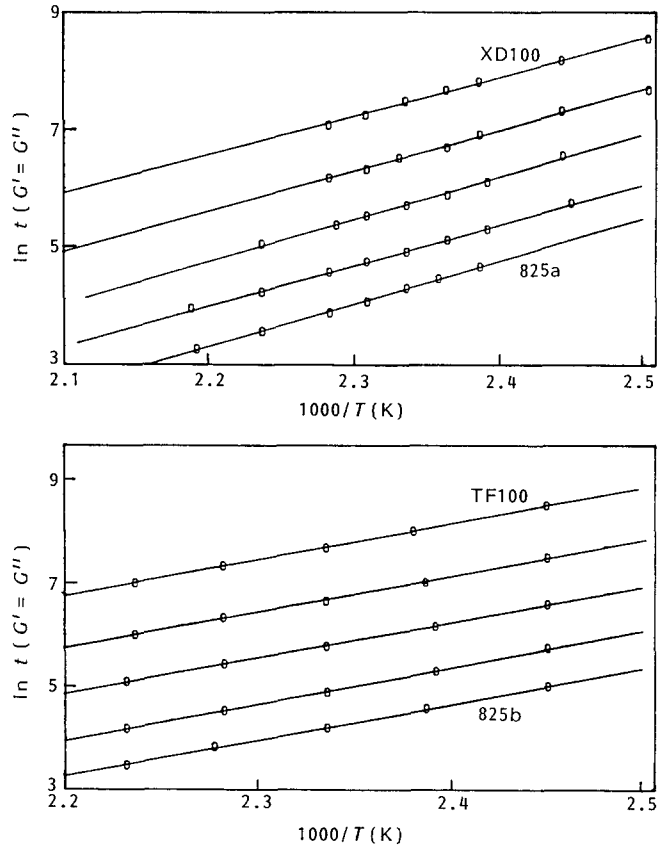

Figure 2 Arrhenius plots for gelation. For clarity, successive plots are displaced along the ordinate by 0, 1, 2, . . ., 4 units

Modelling the curing process

Various quantitative interpretations of viscosity data during cure have been reported. Many have been based on the Williams-Landel-Ferry (WLF) equation[14]:

$$\log_{10} a_T = \frac{-C_1(T - T_s)}{C_2 + T - T_s} \qquad (1)$$

where a_T is the shift factor, T_s is a reference temperature and C_1 and C_2 are constants which are usually given the values of 17.44 and 5.16 respectively if the reference temperature is taken to be the glass transition temperature of the system. This equation was originally proposed to describe the temperature dependence of mechanical and electrical relaxation times of polymers in the region from T_g to about $T_g + 50$°C. Gordon and Simpson[15], however, showed that the rate of increase of T_g at constant temperature, i.e. the rate of crosslinking, for a series of insulating varnishes, was controlled by the mobility of chain segments rather than by chemical structure and that consequently the superposition principle of the WLF equation could be applied to these processes. The rate of reaction is a function of $(T - T_g)$, and as the T_g increases with crosslinking the rate decreases until the T_g reaches the cure temperature when the reaction virtually stops.

Several workers[16–21] have since derived rheological models based on the WLF equation. Two problems arise, however. Firstly, the T_g rises continuously throughout the reaction and secondly the values of the 'constants' C_1 and C_2 vary with degree of cure and composition. Tajima and Crozier[16,17] modelled the curing viscosity of an epoxy–amine formulation using:

$$\log \eta(T) = \log \eta(T_s) - \frac{26.8(T - T_s)}{13.4 + (T - T_s)} \qquad (2)$$

where T_s and $\eta(T_s)$ varied with advancement of the resin and were expressed as functions of the concentration of curing agent reacted. Hou[18,19] related T_g to fractional conversion obtained from d.s.c. experiments, time, cure temperature and the T_gs of the unreacted and fully cured resin. Some authors have combined branching theory and free-volume concepts[20,21]. The former is used to calculate the viscosity in the early stages of cure but, as gelation approaches, molecular mobility becomes more important and the WLF equation is introduced.

Many workers have correlated isothermal data using empirical expressions of the type:

$$\eta = \eta_0 \, e^{kt} \quad \text{or} \quad \ln \eta = \ln \eta_0 + kt \qquad (3)$$

where η is the time dependent viscosity, η_0 is the zero-time viscosity and k an apparent kinetic constant. Roller[22] extended equation (3) to take account of temperature by assuming Arrhenius-type relationships thus:

$$\eta_0 = \eta_\infty \, e^{(E_\eta/RT)} \quad \text{and} \quad k = k_\infty \, e^{(-E_k/RT)} \qquad (4)$$

where η_∞ and k_∞ are the zero-time viscosity and apparent rate constants at $T = \infty$, and E_η and E_k are the associated activation energies. Substituting these two expressions into equation (3) gives:

$$\ln \eta(t) = \ln \eta_\infty + \frac{E_\eta}{RT} + tk_\infty \, e^{(-E_k/RT)} \qquad (5)$$

If the kinetics are assumed to be first order then equation (5) may be converted into a function of time and temperature for dynamic curing data:

$$\ln \eta(T,t) = \ln \eta_\infty + \frac{E_\eta}{RT} + \int_0^t k_\infty \, e^{(-E_k/RT)} \, dt \qquad (6)$$

In order to model the curing viscosity the four parameters $\ln \eta_\infty$, E_η, k_∞ and E_k had to be determined for each material from their semi-log isothermal viscosity profiles. The apparent rate constant was determined at each temperature as the gradient of the log(viscosity) profile in the linear portion before the onset of gelation, according to equation (3). The line was extrapolated to zero time to obtain $\ln \eta_0$. In general all compositions showed increasing rate constants and decreasing zero-time viscosities as the temperature increased. Within each series of mixtures the rate constant and zero-time viscosity at any given temperature increased with resin functionality, although the increases were far more marked for the XD series of blends than for the TF series. There was a large degree of scatter in the zero-time viscosity data, reflecting the difficulty of obtaining accurate values for such low viscosity systems.

Arrhenius plots were then constructed for both $\ln k$ and $\ln \eta_0$ for each system studied, according to equation (4), and linear regression analysis provided values for $\ln \eta_\infty$, E_η, k_∞ and E_k. The values for E_k were in the range 51 to 71 kJ mol^{-1}. The viscous flow activation energies, E_η, were generally very much larger than E_k and showed a wider variation. None of the parameters displayed any consistent effect due to composition.

The four parameters were then substituted into the double-Arrhenius model, equation (6), in an attempt to predict dynamic curing viscosity. In order to test the predictions, a series of dynamic curing experiments was performed on compositions 825, TF 25, TF 50, TF 75 and TF 100. Samples were heated from 70°C to 150°C at 2°C min^{-1} and then held isothermally. *Figure 3* illustrates typical examples of the calculated and experimental curves obtained.

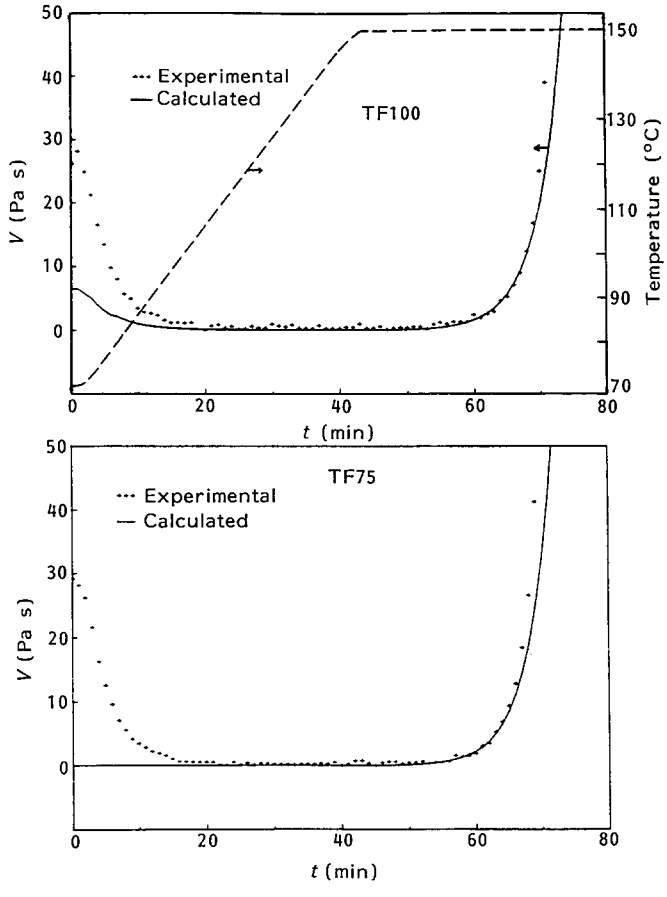

Figure 3 Calculated and measured dynamic viscosity profiles

The model was found to be extremely sensitive to small changes in the viscous flow activation energy, E_η, and slight adjustments of 3 to 4 kJ mol^{-1} or 2 to 4% were made to improve the fit. The correlation between the calculated and experimental curves was poor during the early part of the reaction, and also around the point of minimum viscosity. However, the model was able accurately to predict the onset of a rapid rise in viscosity prior to gelation and thus show some potential as a processing aid. After gelation the predicted curve again diverged from the experimental data.

In an attempt to improve the correlation during the early stages of the cure the zero-time viscosities of the five blends were determined as a function of temperature in the range 30°C to 90°C, where the higher viscosities allowed more accurate measurements. Again there was a marked increase in zero-time viscosity with increasing resin functionality. Arrhenius plots were used as before to obtain alternative values for E_η and $\ln \eta_\infty$. These showed much less scatter than the values obtained from high temperature data and displayed clearly an increase in $\ln \eta_\infty$ and decrease in E_η with increasing functionality.

Using these new values for E_η and $\ln \eta_\infty$ the model was re-evaluated. During the early stages an excellent correlation was seen with the experimental data but unfortunately the fit in the region of gelation was much worse. Clearly the simple Arrhenius-type viscosity equation (4) only holds over relatively short temperature ranges.

Another factor affecting the predictive ability of the model was the low heating rate of 2°C min^{-1}. Both Roller[22] and Tong and Appleby-Hougham[23] have reported that the correlation of the calculated and experimental curves is better at higher heating rates. Furthermore, the systems in the present work were generally of very low viscosity, making experimental measurements during the early part of the reactions very difficult.

Dusi *et al.*[24] extended Roller's model to include the order of reaction, n, and a 'chain entanglement factor', ϕ:

$$\ln \eta(T,t) = \ln \eta_\infty + \frac{E_\eta}{RT} + \frac{\phi}{(n-1)} \times \ln\left[1 + (n-1)\int_0^t k_\infty \, e^{(-E_k/RT)}\, dt\right] \quad (7)$$

The expression only holds when $n \neq 1$. For the purposes of the present work ϕ was set at unity. *Figure 4* shows the calculated curves obtained from this equation for blends TF 100 and TF 50, using the revised values for E_η and $\ln \eta_\infty$. The values of n used are indicated on the diagram. This time the correlation with the experimental data was good, both in the initial stages of cure and in the region approaching gelation.

The six-parameter model used here allowed different values of n to be used, but they are fixed for a given reaction. In practice, the order of reaction may change during the cure, particularly around gelation, as will be seen in the d.s.c. results in the next section. However, to try to adapt the model to account for this would be beyond its limit of applicability since it is based on the simple viscosity relationship (equation (3)), which cannot hold after the gel point.

Overall, the model successfully predicted the onset of gelation for a dynamic curing schedule, using data from isothermal experiments only, in spite of the low viscosity of the systems studied. The model should be applied with caution since it is empirical in nature and takes no account of the reaction mechanism or structural information.

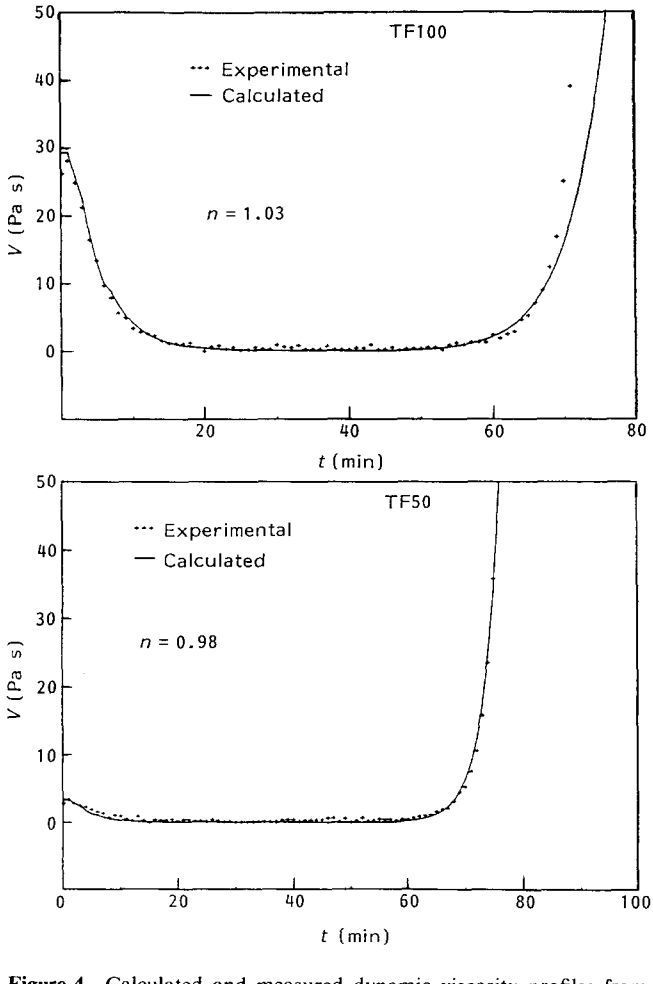

Figure 4 Calculated and measured dynamic viscosity profiles from six-parameter model

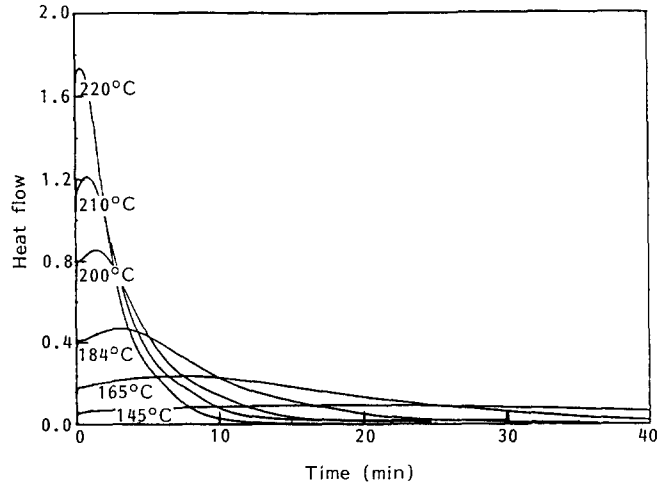

Figure 5 Isothermal d.s.c. curing curves for composition XD 100

Differential scanning calorimetry

Isothermal experiments were carried out on all the compositions listed in *Table 1* at several different temperatures within the range 145°C to 220°C or 250°C for XD 100. *Figure 5* illustrates representative curves for XD 100. The rate of reaction was assumed to be directly proportional to heat flow. The area under each curve was calculated using a trapezoidal summation technique and represented the heat of reaction, Q. *Table 3* lists the heats of reaction obtained for all samples. The values increased with increasing cure temperature until a limiting value was achieved, after which raising the cure temperature further produced no change in the measured heat of reaction, within experimental error. It was assumed that this was because the reaction had proceeded to completion. The total heat of reaction Q_0 was determined by averaging the values for these experiments at 200°C and above. The heat of cure per mole of epoxide, Q', was calculated according to the formula:

$$Q' = Q_0(x + y)E/x \quad (8)$$

where x is the weight of resin, y is the weight of other materials in the mixture and E is the epoxide equivalent weight. In those cases where duplicate runs were performed the reproducibility of the results was found to be between 1 and 5%.

The total observed heat of reaction from isothermal d.s.c. decreased progressively with increasing resin functionality, the effect being far more marked with the XD series of blends than within the TF series. It has been reported[25] for glycidylamine epoxy resins that the

Table 3 Apparent isothermal heats of reaction ($J\ g^{-1}$)

Cure temperature (°C)	Composition								
	825	XD 25	XD 50	XD 75	XD 100	TF 25	TF 50	TF 75	TF 100
250	–	–	–	–	333.1	–	–	–	–
220	401.9	396.7	368.0	355.8	345.3	378.7	376.3	362.0	356.6
210	398.6	378.5	366.1	356.6	340.3	376.3	390.1	342.7	368.7
200	401.3	400.4	378.4	357.5	335.1	392.7	383.3	351.9	351.5
184	374.8	337.9	370.2	349.3	323.3	364.1	372.7	309.9	328.2
165	363.3	368.1	330.3	338.7	328.6	295.5	361.5	257.4	294.0
155	339.2	330.2	315.6	294.2	306.9	274.2	304.2	255.9	283.3
145	236.5	313.1	323.3	257.1	275.6	279.2	288.0	208.3	223.4
Q_0 ($J\ g^{-1}$)	400.6	391.9	370.7	356.6	338.5	382.6	383.2	352.2	358.9
Q ($kJ\ mol^{-1}$)	94.4	90.8	84.6	80.2	75.3	92.0	93.3	86.5	88.7

Table 4 Time (min) to achieve 80% conversion

Temperature (°C)	Composition								
	825	XD 25	XD 50	XD 75	XD 100	TF 25	TF 50	TF 75	TF 100
220	8.0	7.9	6.1	4.8	3.9	7.9	7.5	7.6	6.8
210	12.7	10.4	8.1	6.4	5.2	10.4	10.6	9.4	9.5
200	16.3	15.5	11.3	9.3	7.0	15.5	14.6	12.7	12.3
184	30.9	25.0	19.7	15.4	13.4	25.0	26.8	25.1	26.3

heat of cure per mole of epoxide should be approximately constant since the heat of reaction for epoxy–amine addition is the same as that for the epoxy–hydroxyl group reaction. In the present work, however, there was a significant reduction in Q' with increasing resin functionality, especially for the 825-XD series of blends. It is possible that the differences in the structures of the resins had an effect on the curing process, as will be discussed below.

The ratio of the partial area, Q_t, to the total heat reaction, Q_0, at any time is the fractional conversion, α. Representative plots of α *versus* time for composition 825 are shown in *Figure 6* and illustrate clearly the way in which the rate of reaction and limiting fractional conversion increase with cure temperature. The effect of resin functionality on reaction rates can be seen from *Table 4*, which gives the time to achieve 80% conversion for all blends. Increasing functionality clearly increased the rate of reaction, although the effect was again much more marked for the XD series of blends than for the TF series.

When scanning d.s.c. experiments were performed most blends displayed a broad, single peak, except blend XD 100 which had a slight shoulder on the high temperature side of the peak. The peak temperature for the 825-XD series of blends decreased approximately linearly with increasing functionality from 224°C for blend 825 to 211.5°C for blend XD 100, but little or no change was observed in the peak temperatures for blends of 825 with TF resin. The upper temperature limit of the exotherms was also affected by composition; values ranged from 340°C for composition 825, through 320°C for TF 100 to 290°C for XD 100.

The apparent heats of reaction obtained for all blends are given in *Table 5*, each value representing the average from at least three runs. The trend of decreasing heat of

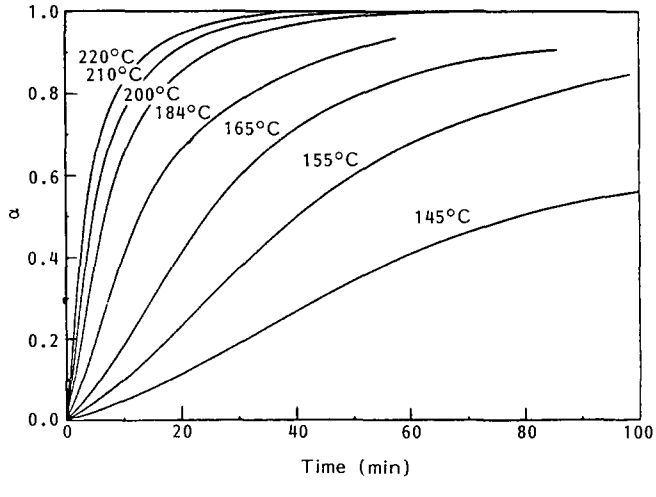

Figure 6 Conversion–time plots for composition 825

cure with increasing average resin functionality was repeated for the scanning experiments, although in the case of the 825-TF series of blends the effect was far more marked in the isothermal results (*Table 3*). It is interesting to note that Naé[6], obtained heats of cure for systems equivalent to compositions 825 and XD 100 of 89.3 $kJ\ mol^{-1}$ and 78.7 $kJ\ mol^{-1}$ respectively, in close accord with the results of the present work, and similar effects have been seen for other systems[26]. The change of the heat of cure with resin functionality suggests that the curing process was not limited to epoxy–amine and epoxy–hydroxyl reactions, which involve the same enthalpy change[25], and that the relative proportions of different reactions was affected by resin composition. Alternatively the networks produced by the resins of higher functionality may have led to some epoxide groups

Table 5 Apparent heats of reaction from d.s.c. experiments at 10 K min^{-1}

	Composition								
	825	XD 25	XD 50	XD 75	XD 100	TF 25	TF 50	TF 75	TF 100
Q_0 (J g^{-1})	382.8	371.8	360.3	358.3	335.3	376.6	372.6	364.2	358.7
Standard deviation	4.9	3.5	4.2	10.2	5.6	6.1	28.2	7.6	6.2
Q' (kJ mol^{-1})	90.2	86.1	82.2	80.5	74.6	90.6	90.8	89.4	88.6
Q' (kJ mol^{-1}) isothermal	94.4	90.8	84.6	80.2	75.3	92.0	93.3	86.5	88.7

being unavailable for reaction, so leading to a lower apparent heat of reaction. More detailed work would be needed to explain this effect fully.

Kinetic analysis of d.s.c. data

A variety of treatments was applied to the isothermal data in the present work. Most models are based on an expression in which the rate of reaction, r, is given by[27]:

$$r = \frac{d\alpha}{dt} = kf(\alpha) \quad (9)$$

where α is the fractional conversion of reactant. If the apparent rate constant, k, is considered to be of the Arrhenius type then it follows that:

$$\ln r = \ln A - \frac{E}{RT} + \ln f(\alpha) \quad (10)$$

where E is the apparent activation energy, T is the temperature, R is the gas constant and A is the pre-exponential factor. The rate of reaction at any time is equal to the heat flow, dq/dt, divided by the overall heat of reaction, Q_0. *Figure 7* shows a typical plot of ln (rate) *versus* $1/T$ for fractional conversions from 10% to 90%. Activation energies obtained in this way averaged 70 to 78 kJ mol^{-1} with no clear trend due to composition. This simple model gives no information concerning the form of the kinetic function $f(\alpha)$.

An expression for nth order processes commonly applied to d.s.c. data is, in terms of α[27]:

$$r = k(1-\alpha)^n \quad \text{or} \quad \ln r = \ln k + n\ln(1-\alpha) \quad (11)$$

where k is an apparent rate constant equal to $k'c_0^{n-1}$, k' is the true rate constant, c_0 is the initial concentration of reactant and n is the order of reaction. The apparent rate constant, k, is only strictly equivalent to k' when c_0^{n-1} is unity, i.e. for first order reactions. For nth order kinetics a plot of ln(rate) *versus* $\ln(1-\alpha)$ should be linear with a slope of n and an intercept of ln k. For the current data all compositions gave plots of the type shown in *Figure 8*.

Up to about 40% conversion the kinetics displayed no fit to the model, the graph being curved. From this point on, however, an approximately linear relationship was seen. Around 80% conversion a gradual change of gradient occurred and the graphs often showed a second linear portion. Linear regression analyses were carried out over all the data from 40 to 94% conversion and for the data in the steepest part of the graph in the range from 55 to 75 $\pm$ 0.05% conversion. The values obtained for the order of reaction, n, and the apparent rate constant, k, over the former range are given in *Table 6*. The best fits to the model resulted in fractional values for n. Each blend showed a gradually increasing order

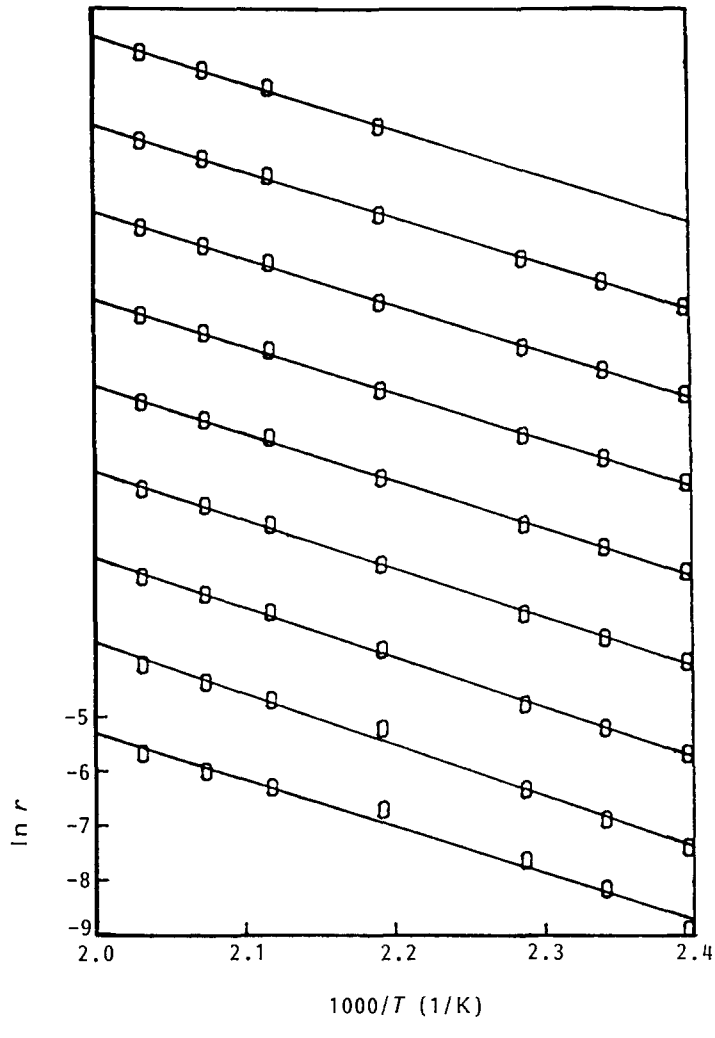

Figure 7 Plots of ln r against $1/T$ for composition XD 50. Successive plots for $\alpha = 0.1, 0.2, \ldots, 0.9$ are displaced along the ordinate by $0, 1, \ldots, 8$ units respectively

of reaction and rate constant with increasing cure temperature. Increasing the resin functionality produced an increase in the rate constant and a decrease in the order of reaction at any given temperature. This effect was much larger for the 825-XD series of blends than for the 825-TF series. Arrhenius plots of ln k *versus* $1/T$ all displayed good linear relationships and the values for activation energies and pre-exponential factors, ln A, are also shown in *Table 6*. Neither displayed any consistent effect due to composition.

In general the nth order model was able to describe quite well the reaction kinetics for all blends from about 40% conversion onwards. The fractional values for reaction order reflected the complexity of epoxy curing

Table 6 Kinetic parameters from $\alpha = 0.40$ to 0.94

	Composition																	
Cure temperature (°C)	825		XD 25		XD 50		XD 75		XD 100		TF 25		TF 50		TF 75		TF 100	
	n	10^3k (s^{-1})	n	10^3k (s^{-1})	n	10^3k (s^{-1})	n	10^3k (s^{-1})	n	10^3k (s^{-1})	n	10^3k (s^{-1})	n	10^3k (s^{-1})	n	10^3k (s^{-1})	n	10^3k (s^{-1})
250									1.14	16.41								
220	1.42	4.61	1.36	5.14	1.21	5.68	1.10	6.28	1.06	7.60	1.30	4.70	1.24	4.70	1.33	4.99	1.24	5.14
210	1.32	3.18	1.46	4.25	1.24	4.25	1.07	4.65	1.01	5.46	1.25	3.48	1.18	3.15	2.25	3.81	1.23	3.74
200	1.28	2.29	1.26	2.61	1.15	2.88	1.12	3.41	0.94	3.85	1.24	2.31	1.18	2.31	1.19	2.74	1.13	2.66
184	1.26	1.15			1.09	1.60	1.06	2.01			1.01	1.19	1.15	1.24				
E (kJ mol^{-1})	71.7		66.0		66.7		60.8		65.7		72.0		68.2		58.0		63.8	
ln A	12.15		10.89		11.15		9.80		11.18		12.26		11.27		8.89		10.32	

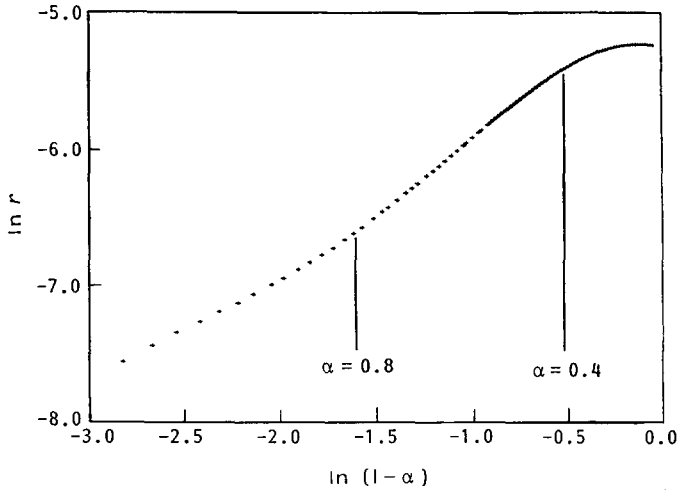

Figure 8 Plot of ln r against ln$(1 - \alpha)$ for composition XD 100 at 220°C

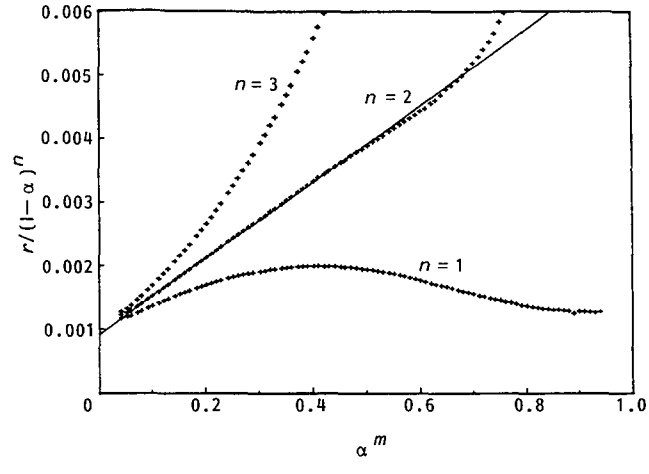

Figure 9 Plots of reduced rate against α^m for composition 825 at 200°C. $m = 1$

reactions and could not be related to a specific step in the curing process. The model was unable to describe the initial stages of the reaction, where the curing process is normally thought to be autocatalytic.

Horie *et al.*[28] derived an expression to describe the autocatalytic kinetics of an epoxy–amine system:

$$r = (K_1 + K_2\alpha)(1 - \alpha)(B - \alpha) \qquad (12)$$

where K_1 and K_2 are rate constants and B is the amine/epoxy molar ratio. A generalized form of this equation has been used by several workers:

$$r = \frac{d\alpha}{dt} = (K_1 + K_2\alpha^m)(1 - \alpha)^n \qquad (13)$$

In the present work this equation was used with $m = 1$ and different integer values for n. *Figure 9* shows representative plots of reduced rate, $r/(1 - \alpha)^n$, *versus* α^m, in this case for composition 825 at 200°C. Plots using $n = 1$ showed a continuously retarding rate and no linear portion or, in the case of composition XD 100, a linear fit over only the first 10 to 20% of reaction. With $n = 3$ all plots displayed a continuously increasing rate. However, when n was set to 2 most blends displayed very good linear relationships up to at least 40% reaction. In general, the quality of the fit decreased with increasing resin functionality and it may be that better correlations would have been obtained in the case of XD 100 and TF 100 if fractional values of n between 1 and 2 had been used.

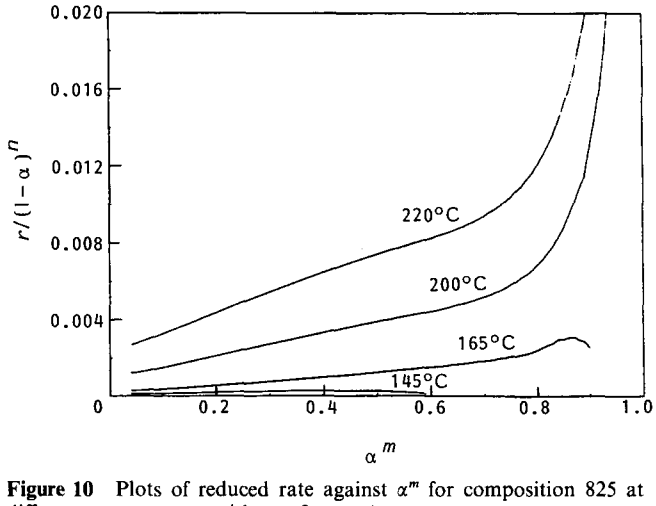

Figure 10 Plots of reduced rate against α^m for composition 825 at different temperatures with $n = 2$. $m = 1$

After about 50 to 60% reaction most plots deviated from the model equation. At higher cure temperatures the graphs showed a slight retardation in rate followed by a sudden increase in the gradient, as shown in *Figure 10*. As the curing temperatures decreased this gradually turned downwards until a marked retardation in rate was seen after 50% reaction at lower temperatures. This would be expected as the viscosity of the system rose and diffusion control became more important. The upward curve at higher temperatures may have been due to

Table 7 Autocatalytic kinetics: apparent rate constants (s^{-1}) × 10^3

Curing temperature (°C)	Composition																	
	825		XD 25		XD 50		XD 75		XD 100		TF 25		TF 50		TF 75		TF 100	
	K_1	K_2	K_1	K_2	K_1	K_2	K_1	K_2	K_1	K_2	K_1	K_2	K_1	K_2	K_1	K_2	K_1	K_2
220	2.41	9.91	2.93	10.75	3.33	11.80	3.81	16.35	4.65	18.77	2.23	10.89	2.40	11.54	2.44	11.48	2.33	13.64
210	1.50	7.85	1.81	9.09	2.24	10.04	2.56	12.00	2.88	13.62	1.30	9.47	1.50	9.44	1.80	9.67	1.46	9.59
200	0.91	6.00	1.14	6.79	1.27	8.17	1.36	9.72	1.96	10.81	0.90	6.36	0.87	6.82	1.16	7.26	1.04	7.82
184	0.50	3.28	0.58	3.97	0.60	4.98	0.73	5.86	0.96	5.95	0.41	4.07	0.45	3.83	0.54	3.80	0.47	3.94
165	0.23	1.73	0.19	2.44	0.30	2.26	0.35	2.79	0.47	3.00	0.20	1.71	0.22	1.91	0.16	1.51	0.19	1.86
155	0.11	1.26	0.14	1.36	0.18	1.58	0.20	1.81	—	—	0.11	1.30	0.12	1.26	0.12	1.23	0.13	1.24
145	0.08	0.62	0.09	0.92	0.10	1.08	0.13	1.05	—	—	0.08	0.08	0.08	0.78	0.07	0.79	0.07	0.74
E (kJ mol^{-1})	77.6	61.3	80.6	56.6	78.4	56.9	76.4	61.7	74.3	59.8	75.9	61.1	76.6	62.2	84.2	64.2	79.1	66.3
ln A	12.9	10.5	13.8	9.4	13.4	9.6	13.0	11.0	12.7	10.7	12.3	10.5	12.6	10.8	14.6	11.3	13.2	12.0

differences in the relative reactivities of primary and secondary amines or may simply be ascribed to the reaction no longer fitting the autocatalytic model; indeed the process from about 40 to 50% reaction onwards seemed to be better described by the *n*th order kinetic model discussed earlier.

The values for the rate constants K_1 and K_2 obtained from these plots are given in *Table 7*. As seen for the *n*th order kinetics, the effect of composition was much greater for the 825-XD series than for the 825-TF series; values of K_1 and K_2 increased by 80 to 110% on going from 825 to XD 100. For compositions 825 to TF 100, however, K_2 increased by 38% at 220°C, decreasing with temperature until no change at all occurred at 155°C and no effect on K_1 was seen at any temperature. Arrhenius plots of ln K_1 and ln K_2 *versus* $1000/T$ showed good linearity and the activation energies and values for ln A are also shown in the tables. As before there was no simple composition effect.

Comparison of chemorheological and d.s.c. data

The complementary nature of chemorheological and calorimetric measurements was demonstrated by the current results. Both techniques showed how an increase in resin functionality produced a corresponding increase in reactivity, and that this effect was consistently more pronounced for the 825-XD series of blends than for the 825-TF series. Furthermore, the relative gel times for certain blends agreed with the relative ranking obtained by Chan *et al.*[2] from torsional braid analysis; i.e. 825 > XD 50 > XD 100.

The empirical nature of the double-Arrhenius viscosity model was reflected in the fact that the values obtained for the apparent rate constants were generally much larger than those obtained from the kinetic analysis of d.s.c. data in the region before gelation, and this effect was also observed by Roller[22]. The overall pattern, however, was the same in both cases, and the model did show some success in the present work in predicting cure behaviour.

The usual explanation for the effect of resin functionality on reactivity is that more highly functional resins have a higher concentration of epoxy groups. From the *n*th order kinetic equation (11) it follows that for a first order reaction the apparent rate constant, k, is equal to the true rate constant, k', and so the concentration of epoxide groups should have no effect. For a second order process $k = k'c_0$ so that any change in c_0 should produce a directly proportional effect on the apparent rate constant, k.

The relative epoxide group concentrations of the resins used in the present work were estimated by calculating the volume of one epoxy equivalent from their epoxide equivalent weights and their densities. On this basis for the most extreme case, i.e. a second order reaction, the apparent rate constant should be approximately 13% higher for XD than for 825, and about the same or even slightly lower for TF resin. However, all the orders of reaction were found to be between 0.9 and 1.5, as shown in *Table 6*. Furthermore the higher viscosity of the higher functionality resins would tend to reduce the rate of diffusion to the reaction site. Both of these would reduce the size of any concentration effect on reactivity. And yet despite this, apparent reaction constants for XD 100 and TF 100 were seen which were respectively 65 to 68% and 11 to 16% higher than those for 825. The autocatalytic model showed increases in K_2 for XD and TF of 80 to 110% and zero to 38% respectively over 825. Clearly, in addition to the concentration of epoxide groups, some chemical effect was also causing differences in reactivity. One possibility is that hydroxyl groups on multifunctional resins, produced as a result of epoxy–amine reactions, may catalyse the reaction of adjacent, unreacted epoxy groups thus reducing the importance of diffusion.

The decrease in gel times observed with increasing functionality was due not only to the higher reactivity of more highly functional resins but also to the fact that they gel at lower fractional conversions[29]. For stoichiometric blends the theoretical conversion at gelation may be calculated according to:

$$\alpha_g = \left(\frac{1}{(f_{A-1})(f_{E-1})} \right)^{1/2} \qquad (14)$$

where α_g is the fractional conversion of epoxide at gelation and f_A and f_E are the functionalities of the amine and epoxide respectively. f_E was weighted for the blends in the present work according to the relative amounts of different resins in the mixture. By combining the rheological and d.s.c. results the experimental values for fractional conversion at gelation, $t_{G'=G''}$, were obtained and these are given in *Table 8*, together with the theoretical values calculated using equation (14).

The experimental values are higher than would be expected from gelation theory, which assumes a perfect

Table 8 Epoxide fractional conversion at gelation, $t_{G'=G''}$

Temperature (°C)	Composition								
	825	XD 25	XD 50	XD 75	XD 100	TF 25	TF 50	TF 75	TF 100
165	0.77	0.71	0.64	0.68	0.73	0.60	0.65	0.46	0.55
155	0.74	0.64	0.62	0.60	0.69	0.61	0.62	0.49	0.52
145	–	0.64	0.62	0.55	0.61	0.61	0.54	0.43	0.43
Theoretical	0.58	0.52	0.47	0.44	0.41	0.47	0.41	0.37	0.33

network. In practice, dangling chains and other network defects are likely to be present. However, the critical conversions followed the trend predicted by gelation theory except for XD 100, which displayed slightly higher values than expected, which could indicate that the XD resin formed a different type of network to the other resin systems. Also some compositions showed higher values at higher cure temperatures. It could be argued that curing at a lower temperature was slower and led to more efficient crosslinking with fewer defects than at a higher temperature. However, the Arrhenius plots for gelation, *Figure 2*, showed very good linearity indicating that a point of constant conversion was being measured. In this light it is likely that the effect was due to experimental differences between the d.s.c. and rheological measurements. In the former case, very small samples were heated rapidly to the isothermal cure temperature. For the rheological work, however, the relatively large samples took longer to equilibrate and during this period the reaction was slower than expected from d.s.c. For the more rapid, higher temperature experiments this period represented a larger fraction of the cure time and so gave higher fractional conversions at gelation. The effect was also more pronounced for higher functionality, more reactive resins.

CONCLUSIONS

D.s.c. and chemorheological measurements were shown to be complementary in the study of epoxy resin cure. The rate of curing increased with increasing average resin functionality, and the magnitude of the effect was shown to be greater than would be expected from concentration effects alone, especially for mixtures containing XD resin, and could be associated with intramolecular catalytic behaviour due to hydroxyl groups. Analysis of d.s.c. data indicated that the kinetics of cure were best described by an autocatalytic model over the first 40% of reaction. Thereafter a simple *n*th order expression gave a better fit to the data.

The use of the modulus crossover point, $t_{G'=G''}$, was found to be a reproducible indication of gelation for the systems studied in this work. Arrhenius plots of ln(gel time) *versus* $1/T$ showed excellent linearity. The fractional conversions at gelation, obtained by combining d.s.c. and rheology data, agreed with the relative ranking predicted from gelation theory, except for composition XD 100. Aspects of the cure viscosity, especially the apparent onset of gelation, were successfully predicted using a theoretical model.

ACKNOWLEDGEMENT

The authors are grateful to Shell Chemicals and Dow Chemical Co. for providing resin samples.

REFERENCES

1 Wright, W. W. *Br. Polym. J.* 1983, **15**, 224
2 Chan, L. C., Naé, H. N. and Gillham, J. K. *J. Appl. Polym. Sci.* 1984, **29**, 3307
3 Peng, X. and Gillham, J. K. *J. Appl. Polym. Sci.* 1985, **30**, 4685
4 Aronhime, M. T., Peng, X. and Gillham, J. K. *ACS Polym. Mater. Sci. Eng.* 1984, **51**, 420
5 Nir, Z., Gilwee, W. J., Kourtides, D. A. and Parker, J. A. *Polym. Compos.* 1985, **6**, 65
6 Hawthorne, K. L. and Henson, F. C. in 'Epoxy Resin Chemistry II', *ACS Symp. Ser.* 1983, **221**, 135
7 Naé, H. N. *J. Appl. Polym. Sci.* 1987, **33**, 1173
8 Mikroyannidis, J. A. and Kourtides, D. A. *J. Appl. Polym. Sci.* 1984, **29**, 197
9 Greenfield, D. C. L. *PhD Thesis*, Brunel University, 1988
10 Barton, J. M. RAE, unpublished work
11 Tung, C.-Y. M. and Dynes, P. J. *J. Appl. Polym. Sci.* 1982, **27**, 569
12 'Standard Test Method for Gel Time and Peak Exothermic Temperature of Reacting Thermosetting Polymers' *ASTM D2471-71* (American Society for Testing and Materials) 1971
13 Winter, H. H. *Polym. Eng. Sci.* 1987, **27**, 1698
14 Williams, M. L., Landel, R. F. and Ferry, J. D. *J. Am. Chem. Soc.* 1955, **77**, 3701
15 Gordon, M. and Simpson, W. *Polymer* 1961, **2**, 383
16 Tajima, Y. A. and Crozier, D. *Polym. Eng. Sci.* 1983, **23**, 186
17 Tajima, Y. A. and Crozier, D. *Polym. Eng. Sci.* 1986, **26**, 427
18 Hou, T. H. 'Chemoviscosity Modelling for Thermosetting Resins', Final Report Nasa-CR-177958, 1985
19 Hou, T. H. SPE Antec '85, 1985, 1253
20 Enns, J. B. and Gillham, J. K. *J. Appl. Polym. Sci.* 1983, **28**, 2567
21 Apicella, A., Nicolais, L., Nobile, M. R. and Castaglione-Morelli, M. A. *Compos. Sci. Tech.* 1985, **24**, 101
22 Roller, M. B. *Polym. Eng. Sci.* 1975, **15**, 406
23 Tong, H.-M. and Appleby-Hougham, G. *J. Appl. Polym. Sci.* 1986, **31**, 2509
24 Dusi, M. R., May, C. A. and Seferis, J. C. in 'Chemorheology of Thermosetting Polymers', *ACS Symp. Ser.* 1983, **227**, 301
25 Barton, J. M. *Br. Polym. J.* 1986, **18**, 37
26 Lau, C. H. *PhD Thesis*, Brunel University, 1985
27 Barton, J. M. *Adv. Polym. Sci.* 1985, **72**, 111
28 Horie, K., Hiura, H., Sawada, M., Mita, I. and Kambe, H. *J. Polym. Sci. A-1* 1970, **8**, 1357
29 Flory, P. J. in 'Principles of Polymer Chemistry', Cornell University Press, Ithaca, New York, 1953, p. 47